Analysis of Flow and Mixing Characteristics of Non-Spherical Particle Mixtures in a Rotating Drum

Muhammad Abdullah, BSc Chemical Engineering

Submitted in fulfillment of the requirements for the degree of Master of Science in Chemical & Materials Engineering

School of Engineering and Digital Sciences

Department of Chemical & Materials Engineering

Nazarbayev University

53 Kabanbay Batyr Avenue,

Astana, Kazakhstan, 010000

Supervisor: Prof. Boris Golman

Co-supervisor: Prof. Sergey Spotar

April 2024

Declaration

I confirm that I am the sole author of the manuscript titled "Analysis of Flow and Mixing Characteristics of Non-Spherical Particle Mixtures in a Rotating Drum," with the exception of appropriately credited quotations and references.

Additionally, I attest to the originality of this work and affirm that it has not been previously submitted for any degree or diploma at Nazarbayev University or any other institution, either in its entirety or in part, at any time before or during its submission.

Name: Muhammad Abdullah

Date: April 30th, 2024

Abstract

This study investigates the flow and mixing characteristics of powder mixtures that incorporate non-spherical particles using both experimental and DEM simulation methods. Investigated particulate materials include Aluminum Oxide (Al_2O_3), Aluminum-Alloy ($AlSi_{10}Mg$), and two composite materials: one composed of 90% $AlSi_{10}Mg$ and 10% Al_2O_3, and the other composed of 95% $AlSi_{10}Mg$ and 5% Al_2O_3. A rotary drum apparatus is used experimentally with different rotational speeds (5, 10, 15, 20, and 30 rpm) to study powder behavior. High-speed videography records the dynamic angle of repose and flow patterns. The results demonstrate a clear correlation between rotation speed and dynamic angle of repose, suggesting that disturbance of the particles increases with higher speeds. Our findings reveal that optimal rotation speeds significantly enhance mixing performance along with best optimized values for achieving a DAOR and promoting mixing efficiency. Three flow regimes, rolling, cascading, and cataracting, are distinguished in the drum due to the effects of rotation speed and particle interactions. Analysis of the segregation index suggests increased rotation speeds enhance mixing efficiency, leading to less particle segregation in composite mixtures. The mixture's composition significantly impacts mixing behavior, as a higher ceramic concentration enhances mixing efficiency. It is critical to regulate rotation speed and particle composition in mixing processes to ensure uniform mixes. This study provides valuable insights into the behavior of powder and the effectiveness of mixing in rotary drums. The work improves comprehension of the parameters affecting powder flow by combining experimental data with DEM models.

Keywords: Powder mixing, Dynamic angle of repose, Non-spherical particles, Rotating drum, Discrete element method simulation, Segregation index, Flow regimes.

Acknowledgments

I want to express my heartfelt gratitude to my diligent mentors, Professors Boris Golman and Sergey Spotar, for their invaluable guidance and support throughout my Master's thesis journey. Their steadfast mentorship and encouragement have played a significant role in the successful completion of my academic program. I am deeply thankful for the countless hours they dedicated to insightful discussions.

Additionally, I wish to acknowledge the administrative team at Nazarbayev University for their behind-the-scenes contributions in creating an enriching academic environment. While their efforts may often go unnoticed, they have been essential in fostering an atmosphere conducive to learning.

Lastly, I would like to express my profound appreciation to my parents for their unwavering encouragement and unwavering support. Their belief in my abilities has served as a constant source of motivation, and I am truly grateful for their presence in my life.

Table of Contents

List of Abbreviations & Symbols

Alphabets

DAOR	Dynamic Angle of Repose
DEM	Discrete Element Method
PEPT	Positron Emission Particle Tracking
PFV-4	Photron FastCam Viewer-4
PIV	Particle Image Velocimetry
RPM	Rotations per Minute

Greek Symbols

α	Lower DAOR
β	Upper DAOR
σ	Deviation

Symbols

F_p	Total force acting on particle *p*
I_p	Inertia moment of particle *p*
T_p	Total torque acting on particle *p*
m_p	Mass of particle *p*
v_p	Translational velocity of particle *p*
w_p	Angular velocity of particle *p*
g	Gravitational acceleration

Compounds

Al_2O_3	Aluminum Oxide
$AlSi_{10}Mg$	Aluminum-Silicon-Magnesium Alloy

List of Figures

List of Tables

Chapter 1 - Introduction

1.1. Background

Granular materials are widely used and, when subjected to force, can retain their structure as a solid or as a fluid flow [1]. The flow of granular material is dictated by several variables, such as particle size and shape. When working with granular materials, the rotary drum is an essential instrument in many processes, such as chemical reaction, sintering, mining, etc. due to its high efficiency, and versatility. Understanding how particles pass through a rotating drum will facilitate its efficient operation at higher speeds. Many studies have been conducted on the flow behavior and mixing process of granular materials [2]. There are two different flow zones in the granular bed of a rotating drum: active and passive. The bed's active region is the area that moves in response to the drum's rotation, whereas the passive layer also moves but with much lower velocities than the particles in the active region. The term "slip surface" describes the boundary that separates the two areas [2]. It is commonly thought that the rolling regime considers stable particle processing, and this is certainly true for most granulation drum operations. As illustrated in **Figure 1-1**, this regime generates an internally circulating D-shaped particle bed.[3]

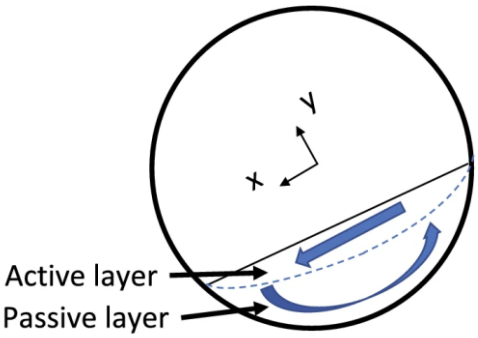

Figure 1-1 A cross-sectional view schematic diagram of a rotary drum in the rolling regime [3].

Particles flow down the sloping bed in the active layer, which is a small lens-shaped flowing zone near the free (flat) surface. Particles move at a high relative velocity in the active layer. The particles in the passive layer do not move like in active region but displace over each other in very low motion [4][5]. Various flow regimes, such as rolling, cascading, cataracting, and centrifuging, are essential for figuring out the dynamics of particles in rotary drums.

At each step, the rotating speed was raised until it reached the centrifuging regime, and granular pictures were recorded. The transition from cataracting to centrifuging was identified by the adhesion of the topmost layer of particles to the dish wall [6]. Particles with steep trajectories during granulation operations increase the likelihood of agglomeration breakdown and fragmentation. The particles start to separate from the equipment wall at the angle of departure (α). Hence, in various flow regimes the angle of departure can be seen in **Figure 1-2** [6].

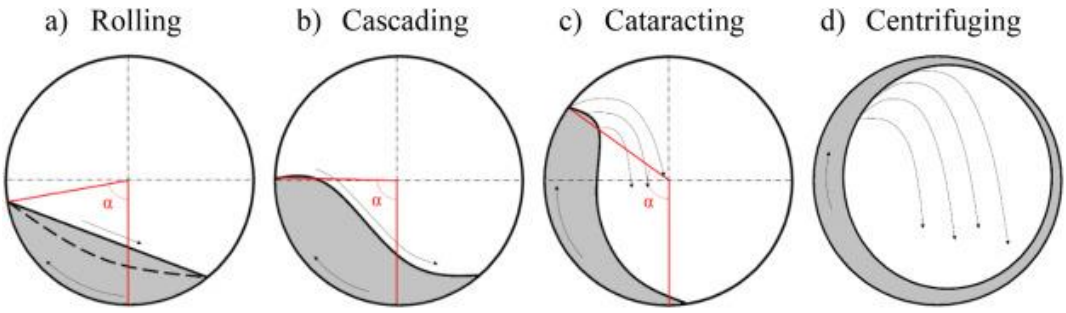

Figure 1-2 Different behaviors of the granular bed investigated in this study and measurement scheme of the angle of departure [6].

Particles with varying densities, particle sizes, and shapes will cause segregation in a rotating drum. Both radial and axial segregation can be achieved in rotating drums of varying sizes. Size-driven and density-driven segregation mechanisms are the most prevalent types of radial segregation in the rotary drum. The percolation effect may separate varying-sized parts in a rotational drum [7]. When this happens, the smallest particles in the flow layer settle into the voids between the bigger ones, creating a core in the bed's center. The size ratio of the particles and volume fraction of the rotating drum are significantly affecting particle movement and segregation degree.

Using the DEM, Huang et al. [8] investigated a binary-size mixture's radial and axial segregation in a long rotational drum. They discovered that size segregation did not affect global parameters like total kinetic energy and the angle of repose. Because of the buoyancy effect [9], particles of varying densities will segregate within a rotational drum. Denser particles penetrate deeper into the granular bed, forming a core, while less dense particles exist closer to the sidewalls of the bed and rest on its surface. Density-induced granular segregation was studied by

Yang et al. [10], who discovered that increasing the volume fraction of powder mixture increased the segregation. It has been found that axial segregation can occur in a rotational drum, possibly because of the disparity between the repose angles of particles. Understanding how granular materials move is often learned through experiments and modeling.

Many experiments, including positron emission particle tracking (PEPT) [11] and particle image velocimetry (PIV) [12], have been done during the past few decades to investigate the flow behavior of granular matter. Experimental study needs to be more comprehensive to examine the mechanism of flow behavior.

Due to its reproducibility and reduced cost, numerical simulation was frequently used to investigate the process of particle movement. Cundall and Strack's DEM is a good illustration of a simulation technique; DEM has developed into a robust methodology for analyzing granular flow in various particle processing equipment, including rotary drums, bladed mixers, intensive mixers, and static mixers [13]. The inter-region behavior and solid residency of granular matter in a rotational drum were investigated by Yang et al. [14], who discovered that bigger particles had more displacement and residence duration and a higher exchange rate between active and passive areas.

This study has some notable gaps, such as not delving into the study of rotating drums with an inclined axis of rotation even though they are present in different industries [15]. Another gap lies in the lack of models to interpret findings on axial segregation in mixtures with multi-spherical particles [16] [17]. Furthermore, more investigation is required to understand how the shape of particles affects flow patterns and the effectiveness of converting energy for non-spherical particles [18]. However, this study investigates the flow and mixing characteristics of powder mixtures that incorporate non-spherical particles using both experimental and DEM simulation methods.

Non-sphericity refers to the deviation of particle shapes from perfect spheres. This deviation can appear in various forms, such as elongation, irregularity, or complex geometries. Non-sphericity is a critical parameter in powder mixing processes as it influences particle-particle interactions, packing behavior, and flow dynamics within the rotary drum. While perfect spheres are often used as a simplifying assumption in theoretical models, real-world powder systems frequently consist of non-spherical particles, necessitating a deeper understanding of their effects on mixing behavior.

1.2. Continuum vs. Discrete Modeling Approach

Continuum models, such as computational fluid dynamics (CFD), treat the powder material as a continuous medium, allowing for the solution of partial differential equations governing fluid flow. On the other hand, discrete element method (DEM) simulations represent individual particles as discrete entities with interactions between them. While continuum models offer computational efficiency and scalability, discrete models provide a more detailed understanding of particle-level dynamics.

1.3. Static and Dynamic Angle of Repose

The angle of repose serves as a fundamental parameter for characterizing the flow properties of granular materials. The static angle of repose represents the maximum angle at which a pile of granular material remains stable under gravity alone, providing insights into the material's cohesion and internal friction. Conversely, the dynamic angle of repose refers to the angle at which granular material flows down a slope under the influence of external forces, such as vibration or rotation.

1.4. Aims and objectives and structure of report

This study aims to investigate the flow dynamics and mixing efficiency of non-spherical particle mixture within a rotating drum. In order to attain these aims, the research is focused on:

- To investigate the dynamic angle of repose for the non-spherical mixtures in the rotating drum.
- To investigate the effects of the drum rotation speed on the mixing and flow pattern.
- To validate the DEM model with experiment for the non-spherical powder mixtures.
- To investigate segregation index for the varying particulate mixtures compositions.
- To study the mixing efficiency for the different non-spherical powder mixtures.

The thesis comprises of five chapters. The first and second chapter provide an introduction and a comprehensive review of relevant literature. These sections explore background, aims, objectives and the prior study related to this work. Following this, the third chapter delineates the methodology, encompassing both experimental and DEM simulation approaches. Subsequently, the fourth chapter presents the results and discussions. Finally, conclusions are drawn in the fifth chapter.

Chapter 2 - Literature Review

Yazdani et al. [19] utilized the DEM to do a comprehensive examination of particle dynamics in a rotating drum. According to their research, the DEM was found to be a more precise representation of the system and highlighted noticeable variations in behavior. The findings of their investigation could be utilized to enhance the design of drums and advance the efficiency of particle handling systems. Memon et al. [20] employed a rotating drum to measure the DAOR of wheat grains. The authors employed a cylindrical drum with dimensions of 20 cm in width and 25 cm in length. The digital camera determined the DAOR by measuring the drum's rotation at different rates. The investigators noted that higher drum speed enhanced the wheat grain DAOR. They an increase in wheat grain DAOR with moisture content, which was consistent with another pattern they identified.

In another experiment, Ribeiro et al. [21] employed a rotating drum to evaluate the DAOR of coffee beans. They had employed a drum measuring 30 cm in width and 40 cm in length. The DAOR was measured using high-speed cameras while the drum was rotated at different rates. The authors found that the coffee beans' DAOR decreased as the drum speed rose. They also noted an increase in the DAOR of coffee beans as their size increased. Shen et al. [22] conducted an experimental investigation on the impact of rotation speed and particle size on the DAOR in a rotating drum. The researchers found that increasing the particle size led to a decrease in the angle. They observed that the particles' DAOR were smaller near the cylinder wall, where the "rolling zone" occurred, due to the weaker centrifugal forces.

Jiang et al. [23] performed experiments to investigate the impact of particle shape on the DAOR in a rotary drum. They validated the findings of Cui et al. [24] that elongated particles have a greater DAOR compared to spherical particles. The authors observed a correlation between the rise in rotation speed and the prominence of the angle of repose. They predicted that this was caused by the increased centrifugal forces exerted on the particles. Kharazmi et al. [25] employed DEM simulations to examine the impact of particle size distribution on the angle of repose within a rotating cylinder. They explored the correlation between a wider range of particle sizes and the angle at which particles come to rest, known as the angle of repose. This investigation focused on how particle size segregation is affected by centrifugal forces.

Yang et al. [26] used the DEM to numerically simulate the movement of particles in a spinning drum across various flow conditions. The authors were able to create six different flow patterns by controlling the rotating speed and the friction between the particles and the wall. These flow patterns include surface flow, centrifuging, slumping, rolling, cascading, and cataracting. The researchers examined both the large-scale and small-scale characteristics of the particle flow, including the angle at which the particles settle, the average speed of the flow, the density, the coordination number, the energy of collisions, and the frequency of collisions. Their research revealed several important discoveries. Firstly, they identified a specific point called the flow density optimum, which represents the most efficient packing arrangement. Secondly, they established a scaling law that describes the distribution of collision energy. Thirdly, they observed that as the rotation speed increased, both the frequency and energy of collisions also increased. Lastly, they noticed a significant increase in the angle of repose in scenarios involving cascading and cataracting.

Alizadeh et al. [27] introduced a particle tracking approach to analyze the mixing and separation of particles in a rotary drum based on their size. In order to track and monitor individual particles, the authors utilized a digital image processing technique following the capture of images of the particle flow using a high-speed camera. The researchers measured the mixing index, radial and axial segregation indices, and particle trajectories for different operating parameters, such as rotation speed, filling degree, and particle size ratio. As the rotational velocity increased, the degree of mixing decreased, but the filling level and particle size ratio exhibited an inverse pattern. In addition, they observed that the paths of particles were influenced by the flow conditions and the size of the particles, and that the separation of particles in the radial direction was more prominent than in the axial direction.

Guo and Curtis [28] conducted a study on DEM simulations of complex granular flows with non-spherical, flexible, cohesive, or fractured particles. Their demonstration highlighted the application of DEM models in studying fluidized beds, pneumatic conveying, hopper discharge, tablet coating, sand dune development, debris flow, and the features and behavior of granular material flow in various natural and industrial processes. The study presented a brief summary of DEM for complex granular fluxes, as well as its future possibilities. Dubé et al. [29] utilized the DEM to investigate the behavior of non-spherical particles in a rotating drum. To examine the flow behavior of spherical and cylindrical particles, various aspect ratios, rotation speeds, and filling degrees of the drum were employed. They computed the mean angles at which materials come to rest, the speeds at which they flow, coordination number, and the amount of

energy transferred during collisions. Upon comparing spherical and non-spherical particles, it was found that the non-spherical particles had higher collision energy and frequency, as well as lower coordination numbers, flow velocities, and DAOR. In addition, they observed that the non-spherical particles exhibited more complex and unusual flow patterns, such as surface flow, cascading, slumping, and rolling. The study conducted a thorough analysis of the impact of particle form on the dynamics of granular flow within a rotating drum.

An additional study conducted by Rasouli et al. [30] investigated the transverse flow velocity and mixing of cylindrical and spherical particles using the multiple radioactive particle tracking (MRPT) technology, similar to the work conducted by Dubé et al. [29]. Alizadeh et al. [27] conducted study that examined the process of mixing and size segregation of spherical and cylindrical particles. They used particle tracking analysis to analyze this phenomenon. This research emphasized the importance and challenges of employing experimental approaches to investigate the flow behavior of non-spherical particles in rotating drums.

The researchers Yari et al. [31] using the DEM to investigate the segregation of bi-disperse granular mixes in a rotating drum. One type of mixture had varying diameters but consistent densities, while the other type had uniform diameters but varying densities. The researchers examined the effects of changing the filling degree, particle size ratio, particle density ratio, and rotation speed on the mechanisms and patterns of segregation. Each case was evaluated based on many metrics, such as radial and axial segregation indices, mixing index, mean flow velocity, and mean collision frequency. The segregation patterns were influenced by the flow regime and particle properties. It was observed that size segregation was more prominent than density segregation. In addition, they observed that the segregation mechanisms were mostly driven by percolation effects and kinetic sieving. The study thoroughly and quantitatively investigated the occurrence of size segregation in bi-disperse granular mixes within a rotating drum.

Kuo et al. [32] utilized the DEM to examine the impact of independent end wall rotations on the segregation of particles in a rotating drum. The study investigated the impact of the rotational speed and direction of the end wall on the size of the shearing zone and the patterns of segregation. They measured spatiotemporal diagrams, radial and axial segregation indices, and the mixing index under various situations. It was found that by creating specific slopes and depressions on the bed surface, rotating the end wall may control the separation of particles, resulting in the formation of convection flow cells and the separation of particles along the axis.

In addition, it was discovered that rotating the end walls could enlarge the shearing zone and result in distinct segregation patterns, specifically two mixed zones located at the end walls. The paper proposed a novel and effective method to manage the segregation phenomena in the rotating drum by adjusting the rotations of the end walls.

Li et al. [33] conducted a DEM simulation to investigate the flow behaviors and mixing characteristics of several sphero-cylinder shapes in a spinning drum, at both macroscopic and microscopic levels. An assessment was conducted to determine the influence of four distinct geometries of sphero-cylinders - spheres, cylinders, prolate spheroids, and oblate spheroids - on the flow dynamics and mixing quality of granular materials. The researchers evaluated various values for the aspect ratio, particle size, filling degree, and rotation speed to determine the impact of these factors on the mixing index, mean collision energy, mean collision frequency, angle of repose, mean flow velocity, and mean coordination number. The researchers found that the flow patterns and ability to mix granular materials were influenced by the morphology of the sphero-cylinders. When comparing spheroids with cylinders, the researchers discovered that oblate and prolate spheroids exhibited flow patterns that were more intricate and asymmetrical. This work conducted a comprehensive and well-structured investigation into the mixing characteristics and flow dynamics of various sphero-cylinder geometries within a rotating drum.

Dubé et al. [29] conducted a study on the behavior of spherical and cylindrical particles with different aspect ratios, rotation speeds, and filling degrees. Their work, similar to that of Li et al. [33], focused on the mixing and dynamics of non-spherical particles in rotating drums. Furthermore, Alizadeh et al. [27] introduced a particle tracking method to investigate the blending and separation of spherical and cylindrical particles. Investigating the flow characteristics and mixing efficiency of non-spherical particles in rotating drums were significant and complex subjects.

Jiang et al. [34] used a DEM to simulate the mixing characteristics of a granular mixture composed of spheres and cylinders in a rotating drum. The authors of this work examined the flow dynamics and mixing quality of a granular system, taking into account several aspects such as the aspect ratio, mass fraction, volume fraction, and rotation speed of the cylindrical particles. They computed the kinetic energy, mixing index, and segregation behavior of the particle for each situation. The researchers found that the flow regime, the interlocking effect, the energy input, and the particle density differential all influenced the quality of mixing. Furthermore, they proposed a quantitative measure for assessing the effectiveness of the sphere-cylinder

combination. This study extensively investigated the characteristics and techniques involved in blending a powder substance consisting of both spherical and cylindrical particles within a rotating drum.

Li and An [35] performed a computational investigation on the blending characteristics and flow dynamics of various tetrahedral shapes in a rotating drum using the DEM. The researchers examined the variations in flow dynamics and mixing quality between granular materials containing tetrahedra and those without them. Additionally, they investigated the disparities between materials that possess elongated and flattened tetrahedra and those that do not. Analyzed were several values for aspect ratio, particle size, filling degree, and rotation speed to ascertain their influence on the mixing index, mean collision energy, mean collision frequency, DAOR, mean flow velocity, and mean coordination number. The shape of the tetrahedra had an impact on the flow regimes and mixing performance of the granular materials. The flow patterns shown by elongated and flattened tetrahedra were characterized by more complexity and unpredictability in comparison to regular and irregular tetrahedra, as seen. This work conducted a comprehensive analysis of the mixing properties and fluid dynamics of tetrahedra shapes in a revolving drum.

The study conducted by Li and An [35] is associated with previous research on the blending and movement of asymmetrical particles in spinning drums. Li et al. [33] utilized DEM to simulate the interaction and mixing of cylindrical forms in a rotating drum. An experimental and computational investigation was conducted to study the mixing properties of a gas-and-liquid two-phase flow using axial-flow.

In reviewing the existing literature [15][17][27][41], it became evident that certain gaps persisted in the study of powder mixing within rotating drums. Two notable gaps include the investigation of rotating drums with an inclined axis of rotation and the absence of models to interpret findings on axial segregation in mixtures with multi-spherical particles. While these gaps represent significant areas for further research, they were not directly addressed in the present study due to several reasons.

Firstly, the focus of this research was primarily on examining the flow and mixing characteristics of powder mixtures containing non-spherical particles within a standard rotary drum setup. The inclusion of an inclined axis of rotation would introduce additional complexities to the system, requiring a separate investigation to thoroughly understand its effects on powder behavior.

Secondly, while axial segregation in mixtures with multi-spherical particles presents an intriguing phenomenon, existing models for interpreting such findings are limited. Developing comprehensive models to interpret axial segregation in these complex mixtures would necessitate extensive theoretical and experimental work. However, it is important to acknowledge these gaps in the literature as they highlight avenues for future research to explore. Investigating rotating drums with inclined axes of rotation and developing models to interpret axial segregation in mixtures with multi-spherical particles could significantly advance our understanding of powder mixing processes and contribute to the optimization of industrial mixing operations.

Previous research has demonstrated that analyzing and assessing the flow characteristics and blending effectiveness of non-spherical particles in rotating drums has been a challenging yet important area of study. Li et al. [33] conducted a DEM simulation to study the flow behaviors and mixing characteristics of different sphero-cylinder shapes in a rotating drum. This study is connected to the previous work by Jiang et al. [34], which focused on analyzing the dynamics and mixing of non-spherical particles in the same system.

Table 1-1 Summarized table of different studies.

Researchers	Parameters	Drum size	Type of Particles	Outcome/Conclusion
Memon et al. [20]	Drum speed, moisture content, DAOR	20 cm width, 25 cm length	Wheat grains	Higher drum speed and moisture content increased DAOR of wheat grains.
Ribeiro et al. [21]	Drum speed, DAOR	30 cm width, 40 cm length	Coffee beans	DAOR of coffee beans decreased as drum speed increased. Larger coffee beans had higher DAOR.
Alizadeh et al. [27]	Rotation speed, filling degree, particle size ratio, mixing and separation	Not mentioned	Spherical and cylindrical particles	Degree of mixing decreased with increased rotation speed. Filling level and particle size ratio had inverse effects on mixing. Particle size and flow conditions influenced particle paths.
Dubé et al. [29]	Rotation speed, filling degree, aspect ratio, flow behavior	Not mentioned	Spherical and cylindrical particles	Non-spherical particles had higher collision energy and frequency, lower coordination numbers, flow velocities, and DAOR compared to spherical particles.
Jiang et al. [34]	Rotation speed, aspect ratio, mass fraction, volume fraction, mixing characteristics	Not mentioned	Spheres and Cylinders	Flow regime, interlocking effect, energy input, and particle density differential influenced mixing quality. Proposed a measure for assessing sphere-cylinder mixing effectiveness.
Yang et al. [26]	Rotating speed, friction, flow patterns, particle properties	Not mentioned	Not specified	Identified flow density optimum, established scaling law for collision energy distribution, observed increased collision frequency and energy with rotation speed, significant increase in DAOR for cascading and cataracting flows.
Shen et al. [22]	Rotation speed, particle size, DAOR	Not mentioned	Not specified (assumed spherical)	Increasing particle size decreased DAOR. Particles near the cylinder wall had smaller DAOR due to weaker centrifugal forces.

Chapter 3 - Methodology

3.1. Research Design

This research explores the flow and mixing properties of powder mixtures consisting of non-spherical particles. To attain a comprehensive understanding, we employed a combined experimental and simulation approach. This strategy capitalizes on the strengths of each method, yielding a more profound and robust analysis compared to solely depending on one method.

3.1.1. Particulate Materials

The particulate materials employed in the present investigation consist of three distinct types: aluminum oxide (Al_2O_3), aluminum-alloy ($AlSi_{10}Mg$), and a composite consisting of 90% aluminum-alloy ($AlSi_{10}Mg$) and 10% aluminum oxide (Al_2O_3). The scanned samples of the aluminum oxide and aluminum-alloy are shown below [36].

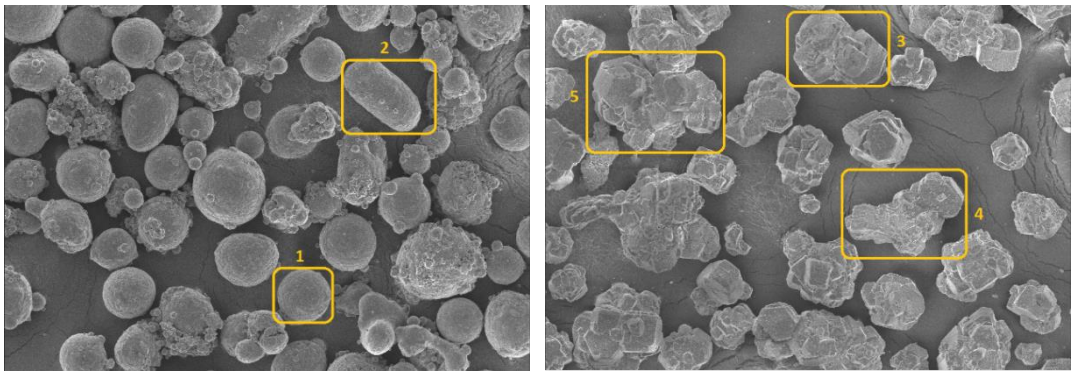

(a) (b)

Figure 3-1 SEM Images of (a) aluminum-alloy particles (b) aluminum oxide particles [36].

Figure 3-1 illustrates the particle shape employed in this study. Specifically, particles labeled as 1 and 2 in **Figure 3-1 (a)** represent spherical and non-spherical particles of $AlSi_{10}Mg$. In **Figure 3-1 (b)**, particles numbered 3, 4, and 5 correspond to small, average, and large particles of Al_2O_3. The diameters of the particles of Al_2O_3 and $AlSi_{10}Mg$ are presented in **Table 3-1**.

Table 3-1 Characteristic diameters of the particles [36]

Property Type	**Alumina**	**Aluminum-Alloy**
$d_{90}\ (\mu m)$	149	70.1
$d_{50}(\mu m)$	99.1	44
$d_{10}\ (\mu m)$	64.4	27

The DEM simulation was employed for the generation of non-spherical particles. While various methods exist for particle generation, this study utilized the multi-sphere method. This approach involves creating non-spherical particles by overlapping spheres with fixed positions. To enhance the precision of the particle model, the shapes of the particles were generated using SEM images of alumina and aluminum alloy particles. This study employed particle simulation to replicate particles as closely as possible to their real counterparts.

Two types of particle shapes were chosen for the aluminum alloy (**Figure 3-1 (a)**): a spherical particle and elongated particles represented by five overlapping spherical particles, as illustrated in **Figure 3-2**. Moreover, a particle model was constructed for alumina utilizing six, eight, and eleven overlapping spheres, as depicted in **Figure 3-3**. This model was designed to closely resemble the scanning electron microscope (SEM) images of these configurations, as illustrated in **Figure 3-1 (b)**.

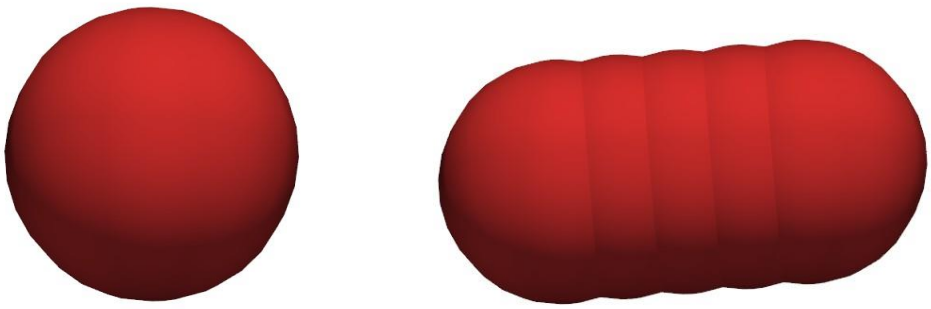

(a) (b)

Figure 3-2 Particle model generated for the aluminum alloy; (a) sphere (b) five overlapping spheres.

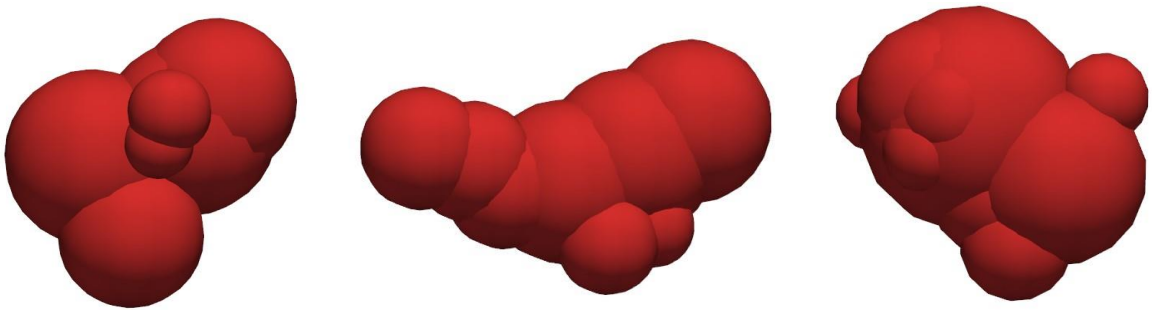

(a) (b) (c)

Figure 3-3 Particle model generated for the alumina; (a) six overlapping spheres, (b) eight overlapping spheres, (c) eleven overlapping spheres.

3.1.2. Rotary Drum

The three-dimensional design of the rotary drum apparatus, illustrated in **Figure 3-4**, comprised a critical and mandatory stage of this study. We employed an aluminum drum assembled specifically for this study. The dimensions of the drum included 200mm diameter and 25mm length. Particularly, the drum featured flat endplates, lacking any baffles or internal flights that could potentially manipulate the powder behavior within the drum.

During the experimental procedure, the drum was filled to a volumetric filling level of 30%. This specific fill level was chosen to represent a practical circumstance commonly encountered in industrial mixing applications. We maintained a constant fill level throughout the experiments to investigate the effect of rotational speed on the powder flow properties. For this study five different speeds of the rotating drum were considered (5, 10, 15, 20, and 30 rpm). Each speed allowed for a more granular investigation of how rotational speed impacted the powder flow characteristics within the drum.

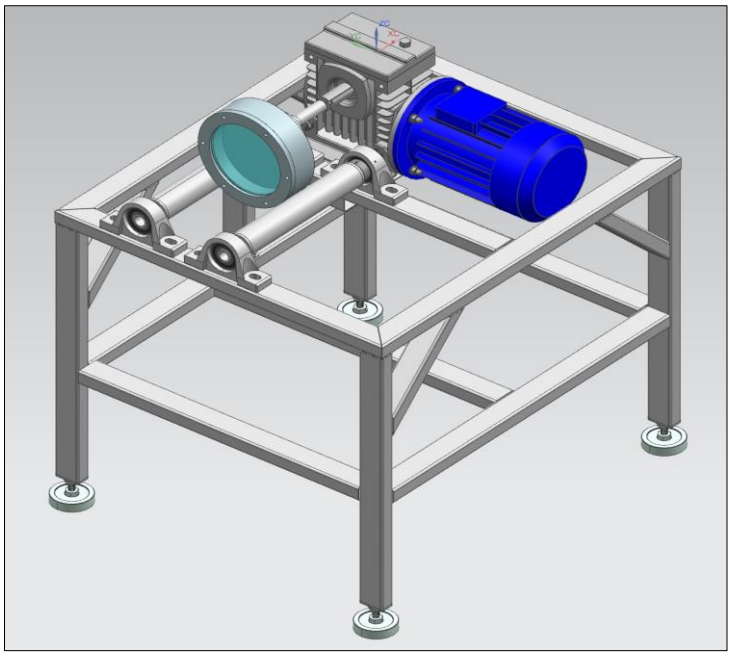

Figure 3-4 Three-dimensional design of the rotary drum apparatus.

For image capture, we utilized a high-speed videography technique employing the SA-Z Full Frame Performance camera. This camera is equipped with advanced capabilities, including a maximum frame rate of up to 480,000 frames per second (fps) for Type 480K, and a minimum exposure of a global electronic shutter to 1μs, selectable independent of frame rate. The camera features a dynamic range of 12-bit monochrome and 36-bit color, ensuring high-quality image capture. With memory capacity options ranging from 8GB to 128GB, it offers ample storage for recording frames at full resolution. The camera control interface supports high-speed Gigabit Ethernet for efficient data transfer. Additionally, the camera is designed for durability, with environmental operating conditions ranging from 0 to 45°C and operational shock resistance tested up to 25G. These specifications ensure reliable and accurate image capture essential for our experimental investigations. This methodology facilitated the subsequent evaluation of both the upper and lower DAOR of the powder bed within the drum, as illustrated in **Figure 3-5**. The DAOR provided valuable insights into the flowability of the powder mixture.

To support and rotate the drum, we applied a system utilizing two rotating rods. These rods were securely attached to a frequency controller, a device precisely designed to regulate and maintain a constant rotational speed. We were able to control the speed of the drum by adjusting the dialer on the frequency controller. For a controlled and uniform experimental environment, allowing a focused analysis of the influence of rotational speed on the flow properties of the powder mixture within the drum.

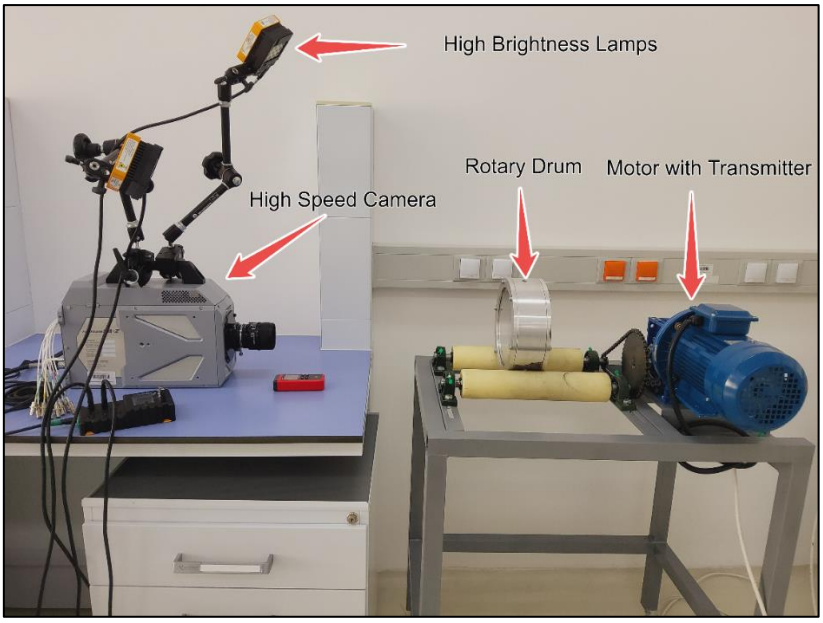

Figure 3-5 Experimental apparatus of rotary drum with high-speed camera.

3.2. Experimental Approach

The experimental approach focused on measuring the DAOR and flowability properties of the powder mixtures using a rotary drum. This technique allows for the observation and quantification of the powder behavior under dynamic conditions like those encountered in various industrial applications.

Three distinct types of powder particles, namely aluminum oxide (Al_2O_3), aluminum-alloy ($AlSi_{10}Mg$), and a composite composed of 90% aluminum-alloy ($AlSi_{10}Mg$) and 10% aluminum oxide (Al_2O_3), were introduced into the rotary drum for three separate experimental trials aimed at quantifying the DAOR and flow pattern at specified rotational speeds. **Figure 3-6** shows the powder particles at initial stage after inserting (0 rpm).

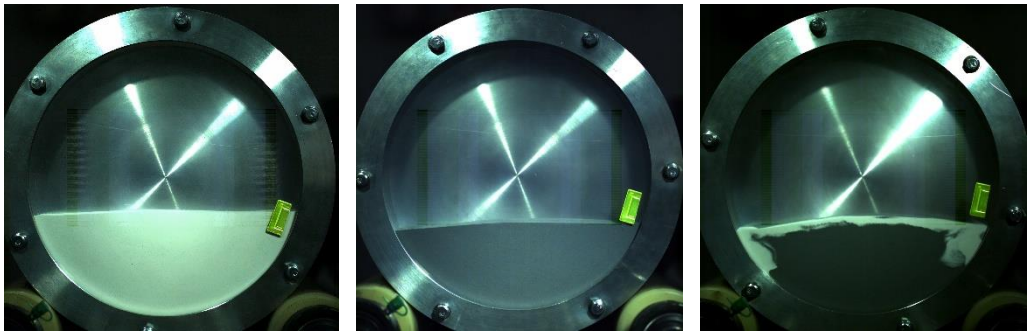

(a) (b) (c)

Figure 3-6 Powder particles at 0 rpm (a) aluminum oxide, Al_2O_3 (b) aluminum-alloy, $AlSi_{10}Mg$ (c) mixture of both Al_2O_3 and $AlSi_{10}Mg$

In the present study, after the insertion of particulate matter, a settling period was allowed. For a filling level of 30% within the rotary drum, the three distinct categories of the powdered materials were weighed as follows: 282.74g for Al_2O_3, 296.23g for $AlSi_{10}Mg$, and 300g for the composite mixture comprising both materials. The experimental apparatus, customized according to our specifications, necessitated the initiation of the experiment by adjusting the motor speed through a dialer. To accomplish this adjustment, a tachometer, employed for measuring the rotational speed of the rotary drum, was utilized. To observe the visual characteristics of the powdered material, a high-speed camera was employed in conjunction with specialized software (PFV-4). The camera parameters were meticulously adjusted to optimize visualization and attain the most discernible results.

Initially, the experimentation commenced with Al_2O_3, involving the adjustment of the drum speed to 5 rpm. The flow pattern of the powder was observed during rotation, and snapshots were captured to quantify the DAOR. Subsequently, identical procedures were applied to assess the flow pattern and DAOR for the remaining two types of powdered materials at rotational speeds of 10, 15, 20, and 30 rpm.

An open-source software ImageJ was employed for the analysis of the results derived from the collected data. This software facilitated the measurement of the DAOR and the assessment of flow behavior for each visual snapshot.

3.3. Numerical Method and Simulation Approach

3.3.1. DEM Model

It is possible to characterize the two kinds of motions; rotational and translational, that each particle exhibits in DEM using Newton's second law [37].

$$m_p \frac{dv_p}{dt} = F_p + m_p g \tag{1}$$

$$I_p \frac{dw_p}{dt} = T_p \tag{2}$$

where m_p, v_p, I_p, w_p, and g are the mass, translational velocity, inertia moment, angular velocity, and gravity acceleration of particle p, respectively, and F_p and T_p are the total force and total torque acting on particle p.

In the multi-sphere model, the total force F_p of each particle p is the sum of forces acting on its element spheres.

$$F_p = \sum_{s=1}^{ns} F_{ps} \tag{3}$$

where ns is the total number of element spheres of particle p, F_{ps} is the force of element sphere s in particle p, and the force of each element sphere can be divided into normal force F_{ps}^n and tangential force F_{ps}^t

$$F_{ps} = F_{ps}^n + F_{ps}^t = \sum_{c=1}^{cs} (F_{psc}^n + F_{psc}^t) \tag{4}$$

where cs is the total number of contact points on each element sphere. The normal force F_{psc}^n and tangential force $F_{psc}^t$are calculated based on the Hertz model and the work of Mindlin and Deresiewicz [38]. The torque T_p is the sum of the following three parts:

$$T_p = \sum_{s=1}^{ns} (T_{tps} + T_{nps} + T_{rps}) \tag{5}$$

where T_{tps} is created by tangential forces; T_{nps} is created by normal forces when the normal force of the element sphere does not pass through the center of the particle; and T_{rps} is the rolling friction torque. Three different torques T_{tps}, T_{nps}, and $T_{rps}$are given by:

$$T_{tps} = \sum_{c=1}^{cs} (r_{psc} \times F_{psc}^{t}) \quad (6)$$

$$T_{nps} = d_{ps} \times F_{ps}^{n} \quad (7)$$

$$T_{rps} = \mu_r |F_{ps}^{n}| \frac{w_p^t}{|w_p^t|} \quad (8)$$

where r_{psc} is the vector between the contact point c and the center of element spheres of particle p and d_{ps} is the relative position vector between the centroid of particle p and the center of the element spheres, while μ_r is the coefficient of rolling friction.

3.3.2. Simulation Approach

The DEM simulation approach was utilized to model the individual interactions between non-spherical particles within the powder mixture. The software was employed for simulating three distinct cases:

I. Al_2O_3 particles

II. $AlSi_{10}Mg$ particles

III. Composite of $AlSi_{10}Mg$ (90 wt.%) and Al_2O_3 (10 wt.%)

Table 3-2 delineates the properties of the powder particles utilized in this study. These properties have been selected to closely align with the properties for conducting the DEM simulation.

Table 3-2 Material properties for the powder particles [36]

Material property	**$AlSi_{10}Mg$**	**Al_2O_3**
Density (kg/m^3)	2230	3800
Young's modulus, G (Pa)	7e6	3.2e7
Poisson's ratio, v	0.3	0.23
Coefficient of restitution, e	0.75	0.4
Coefficient of friction, μ	0.5	0.6
Coefficient of rolling friction, μ_r	0.5	0.005

In this study, the following three phases of DEM simulations were conducted:

Insertion Phase: The initial stage of the DEM involved the introduction of powder particles into the rotary drum, as depicted in **Figure 3-7**. This figure, generated by the visualization software OVITO, provides a snapshot of the particle distribution within the drum at the beginning of the process. During this introduction phase, the particles were characterized by a state of random free-fall, driven solely by the force of gravity. This free-fall resulted in an initial, unordered arrangement of the particles throughout the drum's volume. To achieve a desired volumetric filling of 30%, a specific number of particles were introduced: 5912 Al_2O_3 particles, 6466 $AlSi_{10}Mg$ particles, and for the composite particles, which combined both Al_2O_3 and $AlSi_{10}Mg$, were introduced into the drum based on the weight percentage of five particles proportions shown in **Table 3-3**. This precise control over the number of particles ensured a consistent starting point for analyzing the flow and mixing behavior within the rotating drum.

Table 3-3 Number-based composition of powder particles in the composite mixture

Particle Clump Type	$AlSi_{10}Mg$ (Elongated)	$AlSi_{10}Mg$ (Sphere)	Al_2O_3 (Average)	Al_2O_3 (Big)	Al_2O_3 (Small)
Proportion in composite	0.55	0.35	0.04	0.03	0.03

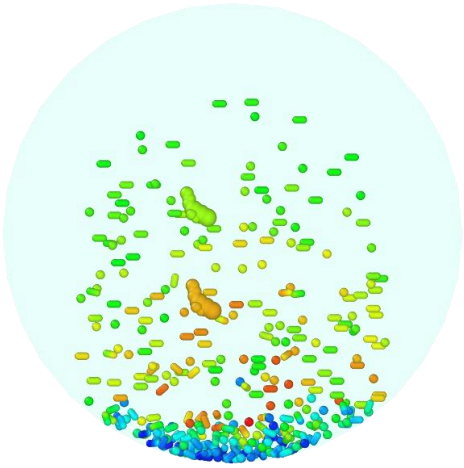

Figure 3-7 Visual of powder material during insertion.

Settling Phase: Following the insertion process, the powders undergo a crucial settling phase, depicted in **Figure 3-8**. During this period, the individual particles, initially disrupted by the insertion, experience a descent and rearrangement. This descent is not simply a haphazard fall, but rather a process that leads to a more uniform and densely packed bed. This phase is critical for establishing a stable starting point for the following dynamic actions within the rotating drum. Imagine this settling phase as setting the stage for a play. The particles need to settle and form a uniform layer to ensure consistent and anticipated behavior during the dynamic mixing processes that follow. This settling phase allows all the particles to rest and find their initial positions within the drum, creating a stable foundation for the complex flow and mixing phenomena to unfold.

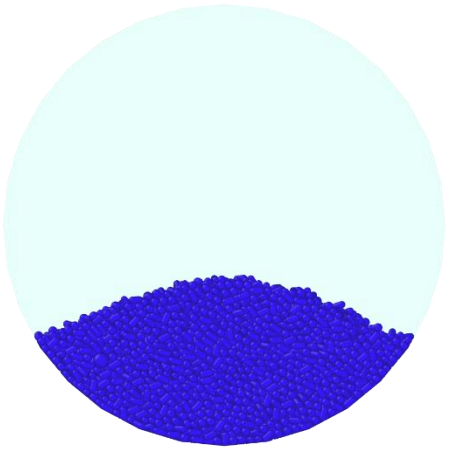

Figure 3-8 Settling phase of the powder material.

Rotation Phase: As the drum-initiated rotation (**Figure 3-9**), the powder mixture within entered in this phase characterized by a confluence of flow regimes. The rotational force imparted a complex direction on the particles, inducing them to not only roll and cascade along the drum's interior surface, but also to participate in cataracting regime. This dynamic interplay between the particles, fostered by the drum's movement, was paramount for assessing the behavior of the powder mixture under these operational conditions. Throughout this critical interval, observations were conducted to capture the evolving relationship between the DAOR, and the flow patterns exhibited by the powder materials. The drum's rotational speed was systematically varied to discern the influence of this parameter on the powder's dynamics. To facilitate the subsequent quantification of the observed phenomena, multiple snapshots were captured for each of the three distinct powder materials under investigation.

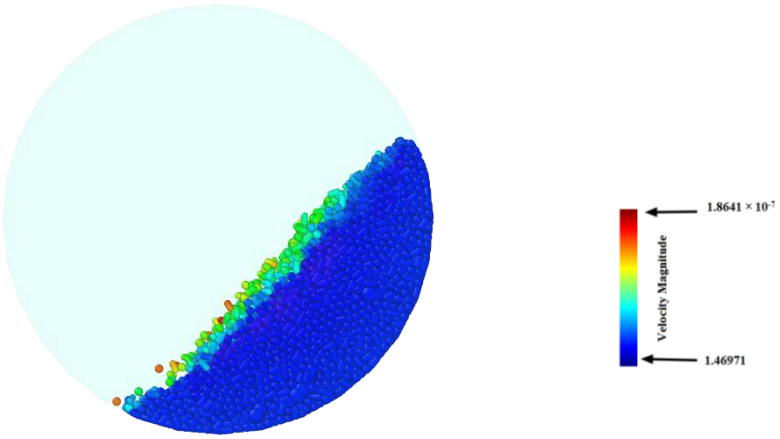

Figure 3-9 Rotation phase of the drum.

3.3.3. Validation of DEM

The verification of data in this investigation constituted an essential element in ensuring the dependability and precision of the results. The all-validation criteria implemented contain the utilization of the DEM simulations and the analysis of the flow behavior of the powder mixture within the rotary drum. This approach was fundamental to establishing the credibility and strength of the investigation, thereby contributing to the advancement of knowledge in the field. One of the primary parameters examined during validation is the DAOR [39], indicated by both the lower angle (α) and the upper angle (β) of the powder mixture, as demonstrated in **Figure 3-10**.

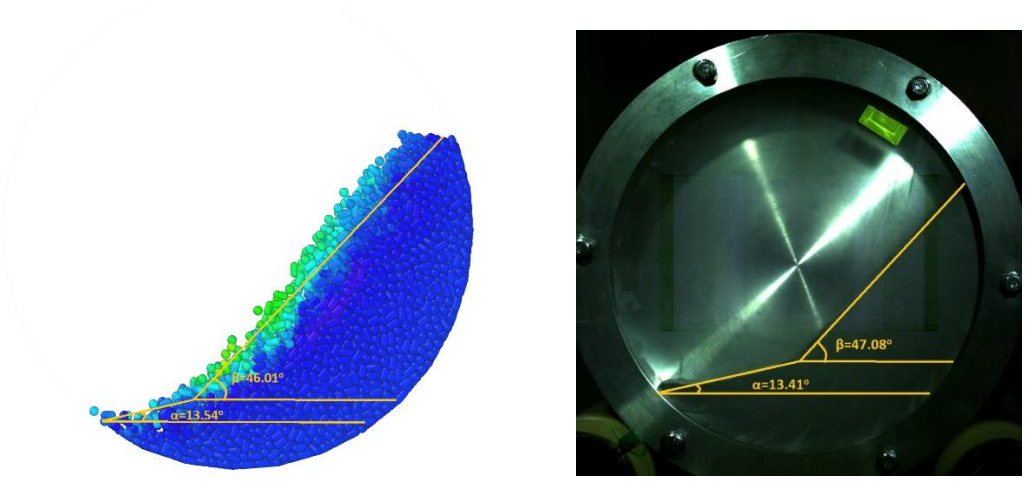

(a) (b)

Figure 3-10 Comparison of both (a) DEM, (b) experimental data for powder mixture with 90% of $AlSi_{10}Mg$ and 10% of Al_2O_3.

The 15rpm rotation speed of the drum provided an approach to validating the process, by ensuring a thorough analysis of the behavior of the powder under controlled conditions. The consistency of this validation process is an important aspect, demonstrated by the selection of powder materials and close to drum dimensions in both DEM simulations and experimental work. This step was essential for removing factors and facilitating a comparison of the results derived from DEM and experimental data.

Nevertheless, it is essential to recognize the inherent constraints arising from the disparity in the quantity of particles employed in simulations as opposed to the actual real-world situation. The issue of accurately depicting the experimental conditions in the simulations was resolved by carefully considering the distribution of particle sizes, taking into account the filling ratio, verifying and adjusting the simulations based on experimental data. These metrics collectively guarantee that although the simulations may not precisely replicate the experimental setup in terms of particle count, they accurately depict the fundamental behaviors and dynamics of the powder mixture within the rotary drum, hence offering useful insights into the system's behavior.

The graph depicted in **Figure 3-11** illustrates the trend lines corresponding to the α and β angles at a specified drum speed. Within the scope of this investigation (**Table 3-4**), the α DAOR obtained through the DEM simulation is recorded as 13.54°, while the experimental counterpart yields a value of 13.41°. Consequently, the absolute error for α is computed at 0.96%. Similarly, comparison of the β DAOR values between the DEM and experimental data revealed measurements of 46.01° and 47.10°, respectively, with an associated absolute error of 2.40% for the β DAOR.

Table 3-4 Comparison of lower and upper DAOR of both DEM and experiment data

RPM	**DEM DAOR (α)**	**Experiment DAOR (α)**	**Absolute error for α (%)**	**DEM DAOR (β)**	**Experiment DAOR (β)**	**Absolute error for β (%)**
15	13.54	13.41	0.96	46.01	47.10	2.40

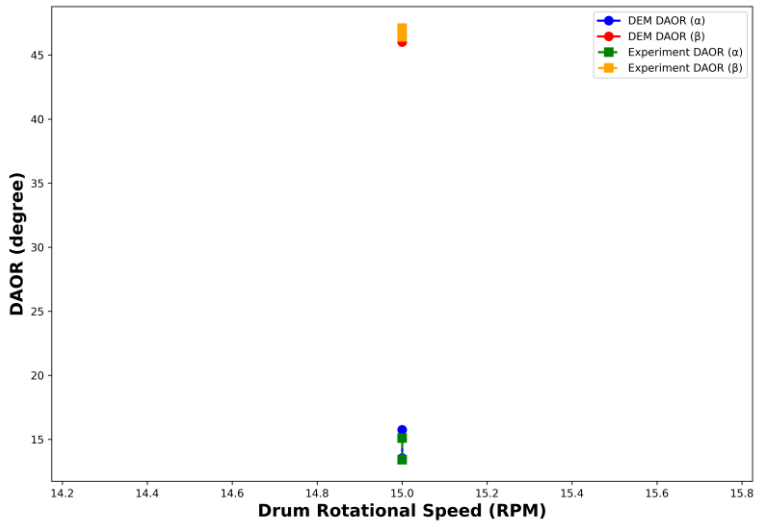

Figure 3-11 Graph to validate DEM and experimental data for powder mixture with 90% of $AlSi_{10}Mg$ and 10% of Al_2O_3.

The indicated speed of 15rpm for validation served as a representative parameter, allowing for a thorough examination of the response of the powder mixture to rotational forces within the drum. This method not only confirms that the results can be reproduced, but also assists a good comprehension of the involved relationship between rotation speed and powder behavior. **Figure 3-10** also demonstrated the flow regime of the powder mixture within the drum, by observing the behavior of the material with open-source software ImageJ. The flow pattern of the powder material at 15rpm is cascading in both DEM simulation and experiment.

Chapter 4 - Results and Discussion

4.1. Flow Characteristics

The investigation aimed to gain a comprehensive understanding of the experimental outcomes by examining the intricacies of the DAOR at different rotational speeds of the rotary drum. The baseline for this exploration was carefully established by setting the fill level of the drum at 30% of its total volume. The initial parameters were configured with great attention to detail, providing a systematic approach to studying the behavior of the powder.

Table 4-1 visually represents the experimental investigation and captures the dynamic responses of the powder at five different speeds. Alterations in the rotational speed of the drum had a noticeable impact on the flow pattern of the particulate material.

Table 4-1 Experiment screenshots of the three different kinds of the powder particle mixture at different speeds

Drum Speed	**5 Rpm**	**10 Rpm**	**15 Rpm**	**20 Rpm**	**30 Rpm**
Al_2O_3	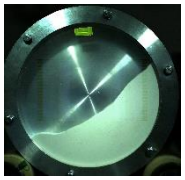	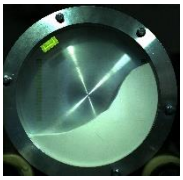			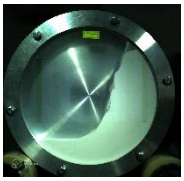
$AlSi_{10}Mg$	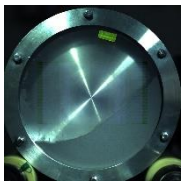	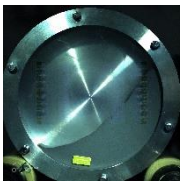	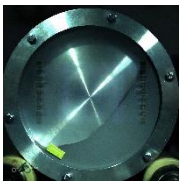	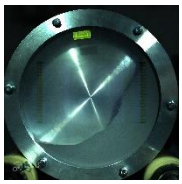	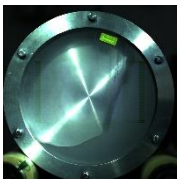
Mixture of Al_2O_3 and $AlSi_{10}Mg$	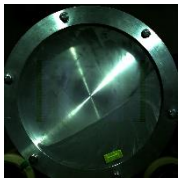	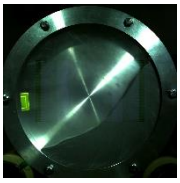	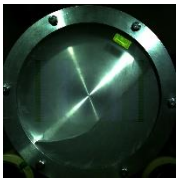	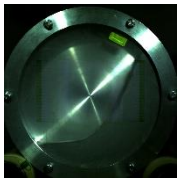	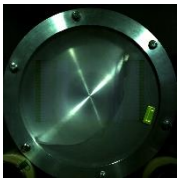

In this experimental study (**Table 4-1**), observed that with increment in the rpm of the drum the powder materials gave different patterns. The ceramic material (Al_2O_3) demonstrated the higher DAOR compared to the other powder materials.

An interesting observation appeared as the rotation speed increased – there was a proportional increase in the DAOR which was measured by image analysis. **Figure 4-1** clearly demonstrates this correspondence, highlighting the direct influence of rpm on the particles. This empirical relationship highlighted the dynamic interplay between rotational dynamics and powder behavior within the rotary drum.

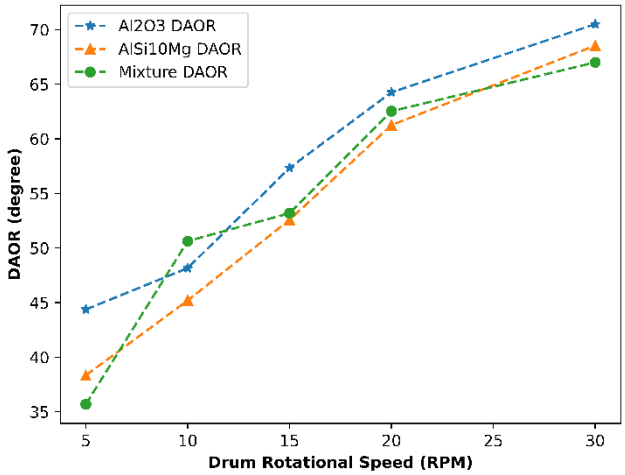

Figure 4-1 DAOR for all the three kinds of the powder materials.

Figure 4-2 illustrates the α and β angles of the particulate materials in all cases. As the rotational speed of the drum increases, α decreases due to the heightened centrifugal force acting on the powder mixture. Consequently, at higher speeds, particles tightly pack against the drum wall, leading to a decrease in α. Meanwhile, at the top of the powder bed, particles experience less compaction, resulting in an increase in β. The findings presented in this study align with the results reported in [40][41] relevant to the DAOR of the powder materials.

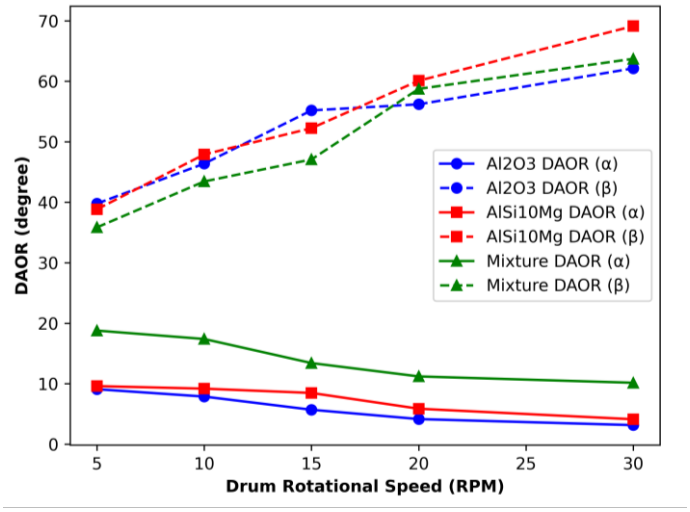

Figure 4-2 Lower and upper DAOR for all three kinds of powder materials.

In a systematic investigation, the flow regimes adopted by the powder within the rotary drum were carefully examined. **Table 4-2** serves as a key illustration, detailing the profound influence of drum speed on the behavior of the granular bed. This investigation focused on three distinct flow regimes: rolling, cascading, and cataracting. The rotational speed of the drum was systematically increased in incremental steps until the cataracting regime was achieved. At each incremental speed, granular images were captured by the high-speed camera, providing a source of data for analysis. This thorough approach allowed for the identification and characterization of the dominant flow regimes on different operating conditions inside the rotary drum.

Within a rotating drum, the behavior of the powder material transforms with increasing rotation speed. At normal speeds, particles interact through rolling and sliding, forming a gentle "rolling regime" where they move over each other [42]. As the drum spins faster, however, centrifugal forces take hold. This stronger force causes the powder to lift and fall, transitioning the flow to a more turbulent "cataracting regime" characterized by cascading particles [43]. The interplay between particle interactions and centrifugal forces directs the flow regime within the rotating drum.

Table 4-2 Different flow behaviors of the powder particles

Speed	**5 Rpm**	**20 Rpm**	**30 Rpm**
Flow behavior	Rolling	Cascading	Cataracting
Aluminum Oxide	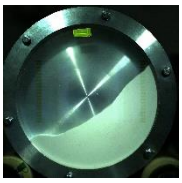	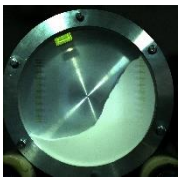	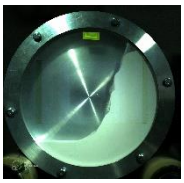
Aluminum-Alloy	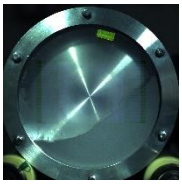	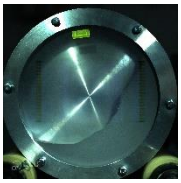	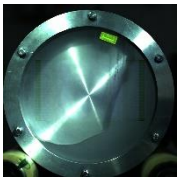
Composite of Al_2O_3 and $AlSi_{10}Mg$	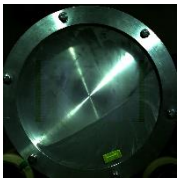	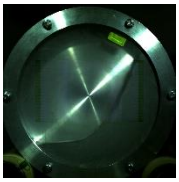	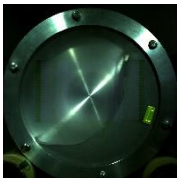

Table 4-3 shows the DEM simulation with the filling level which is same as previously detailed in the experimental section, at 30% of rotary drum's volume. For Al_2O_3, a total of **5912** powder particles were introduced into the rotating drum to achieve the specified filling level. The alumina powder consisted of 50% multi-spherical particles, comprising eight overlapping spheres. The remaining two varieties of alumina powder particles, characterized by six and eleven spheres, were evenly distributed, each constituting 25%. Furthermore, in the case of $AlSi_{10}Mg$, a total of **6466** powder particles were introduced into the drum. The Al-alloy powder comprised 60% spherical particles and 40% elongated particles. The DEM simulation was conducted for a composite powder mixture comprising 90% aluminum alloy and 10% alumina. In this scenario, the total number of particles was **10642**, aimed at achieving a filling level of up to 30%.

The dynamics of powder mixtures in rotary drums is demonstrated in **Table 4-3**, wherein the presence of active (light green color) and passive layers (blue color) is observed to have an effect. The active layer, situated on the surface of the powder bed, exhibits a consistent flow of particles with considerable velocities.

Table 4-3 DEM simulations of all three types of the powder particles

Rotational Speed (rpm)	Al_2O_3	$AlSi_{10}Mg$	Mixture of $AlSi_{10}Mg$ and Al_2O_3
5	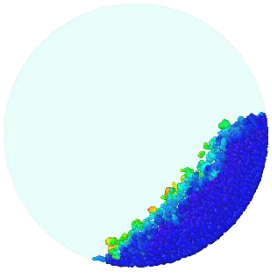	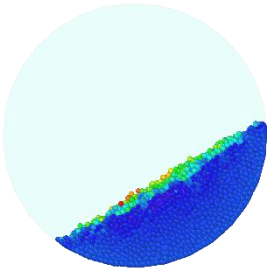	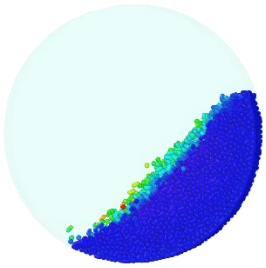
10	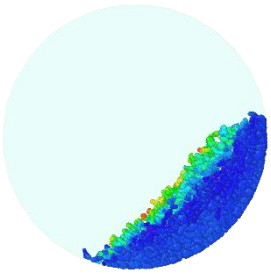	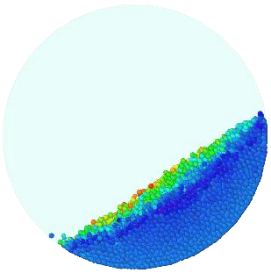	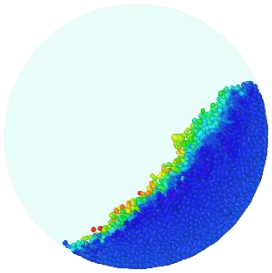
15	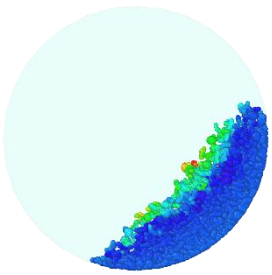	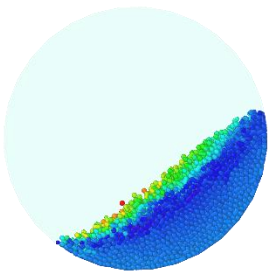	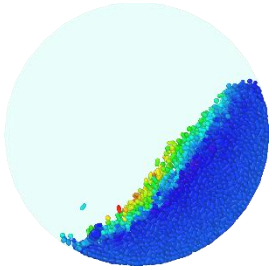
20	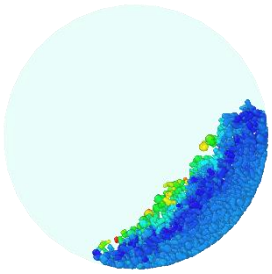	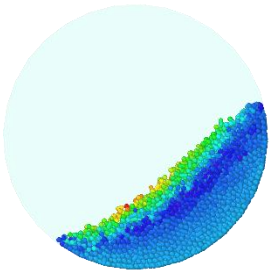	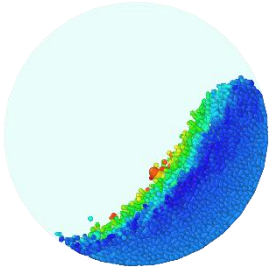
30	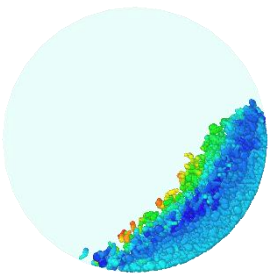	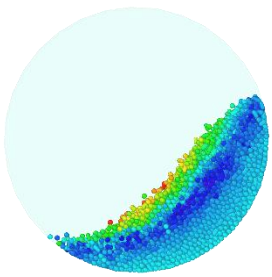	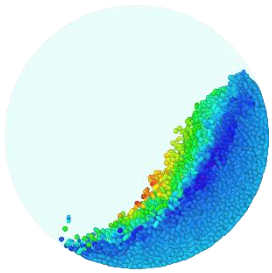

Conversely, the passive layer, positioned in close proximity to the drum wall, displays elevated particle concentrations and reduced velocities. The velocity profiles in the active and passive layers exhibit distinct patterns, where the duration of particle circulation decreases as the rotation speed and drum diameter increase and increases when the fill ratio increases. These patterns agree with the observations in [44][45].

4.2. Mixing Characteristics

The mixing properties of the multi-spherical mixtures were investigated by the segregation index [46]. The segregation index, I_s is defined as :

$$I_s = \frac{\sigma}{M_1} \tag{9}$$

where σ is the deviation of the concentration of the component at different sampling, and M_1 is the initial concentration.

$$\sigma^2 = \frac{1}{n-1}\sum_{j=1}^{n}(M_{1j} - M_1)^2 \tag{10}$$

In this study, we analyzed two different cases of the composite powder mixtures, with 90wt.% of $AlSi_{10}Mg$ and 10wt.% Al_2O_3 while the other mixture with 95wt.% $AlSi_{10}Mg$ and 05wt.% of Al_2O_3. The speeds of the rotary drum in these cases were also the same (5, 10, 15, 20, and 30 rpm). Many factors such as drum size, particle shape, rotational speed, and powder material composition make effect on the powder particles segregation in the rotary drum, which is related with the observations according to [47].

The DEM simulation for the mixture (90:10) visualized in **Figure 4-3**, the parameters for this case were the same as for the other cases discussed in this study. The particles of the powder mixture were initially introduced into the drum in a randomized manner, representing a mixed state. Subsequently, a settling period was provided to allow the particles to arrange themselves. The snapshots were taken for different mixing times at 30 rpm of the drum with the same filling level, 30%. Initially when the rotation started, the bed of the powder mixture created the rolling

regime for the 30 rpm for the 1-second mixing time, but gradually the bed changed the flow regime to cataracting up to the 4-second mixing time.

The case was analyzed to determine the segregation index for the mixture (90:10). At the 1-second mixing time, the larger or denser particles moved outward in the bed, which led to segregation. Conversely, as the mixing time was increased to 4 seconds, the particles were mixed, resulting in a decrease in the I_s. As the composition of the Al_2O_3 was 10 wt.% in this case, which promoted higher content of the ceramic material and helped to achieve better segregation index. Because the higher ceramic contents led to more even distribution throughout the bed of the powder mixture.

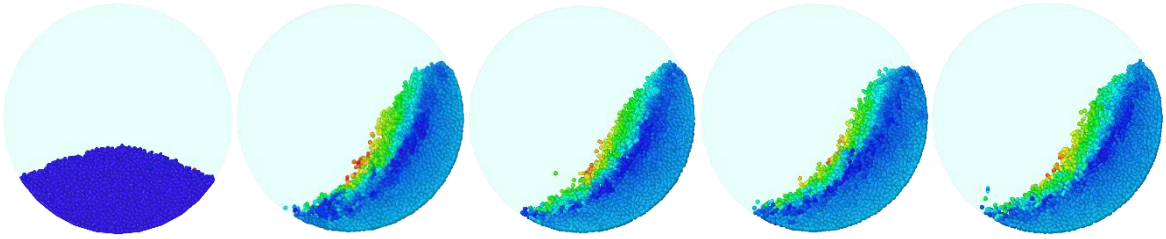

(a) 0-sec (b) 1-sec (c) 2-sec (d) 3-sec (e) 4-sec

Figure 4-3 DEM simulation visuals of the mixture (90:10) at 30 rpm for different mixing times.

In **Figure 4-4**, the segregation index of the composite mixture (90:10) was examined at various mixing times (0, 1, 2, 3, and 4 seconds) within the rotary drum. The graph presented a relationship between the drum's rotation speed (rpm) and the segregation index. Data for each rpm setting was collected using DEM simulation at five distinct mixing time intervals. A trend arisen from the results depicted in **Figure 4-4**. As the rpm of the drum increased, a consistent decrease in the segregation index was observed. This indicated that higher rotation speeds promoted more effective mixing, leading to a more uniform distribution of the Al_2O_3 particles within the composite mixture. In other words, the higher speeds counteracted the inherent tendency of the components to separate during the mixing process.

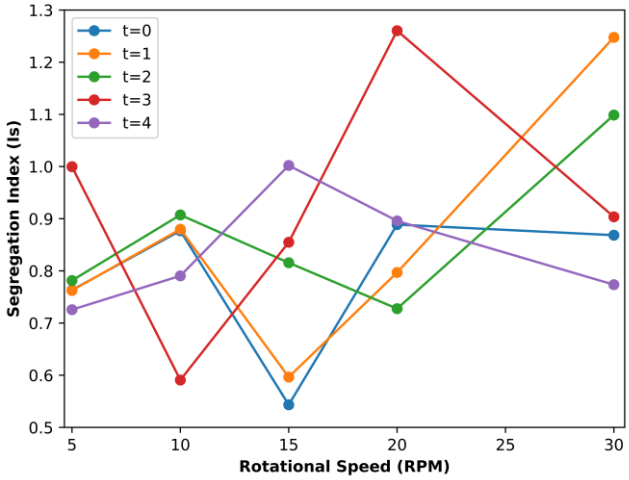

Figure 4-4 Segregation index for the mixture 90:10 at different mixing times.

Figure 4-5 showed the DEM simulation for the mixture (95:05), in which the total number of particles was higher than in the previous scenario, totaling 10,720. This difference in particle count contributed to variations in the segregation index, particularly due to the lower ceramic content compared to the previous scenario. Consequently, the particles required more energy to achieve a uniform distribution throughout the bed, resulting in lower segregation index values, as documented in [48].

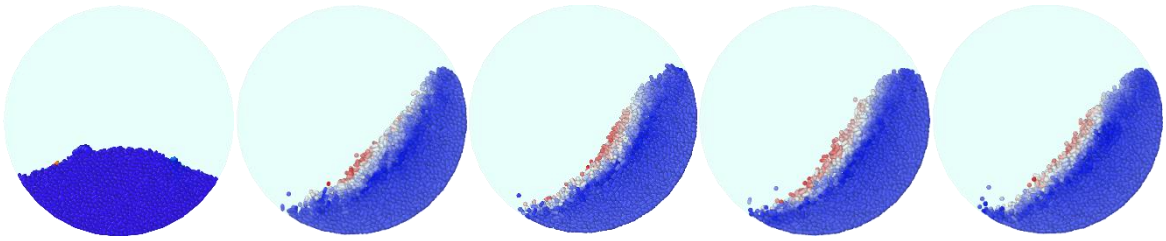

(b) 0-sec (b) 1-sec (c) 2-sec (d) 3-sec (e) 4-sec

Figure 4-5 DEM simulation visuals of the mixture (95:05) at 30 rpm for different mixing times.

As illustrated in **Figure 4-6**, the segregation index for the 95:5 powder mixture within the rotating drum exhibited a clear correlation with mixing time. At the outset, with zero mixing time, the segregation index was high. This signified a poorly mixed state for the powder

components. However, as mixing time progressed up to 4 seconds, a significant decrease in the segregation index was observed. This trend indicated a continual improvement in the mixing quality of the powder. In other words, the powder particles progressively distributed more evenly throughout the mixture as the mixing time increased. This suggested that the rotating drum effectively promoted the mixing process, overcoming the initial separation tendencies of the components.

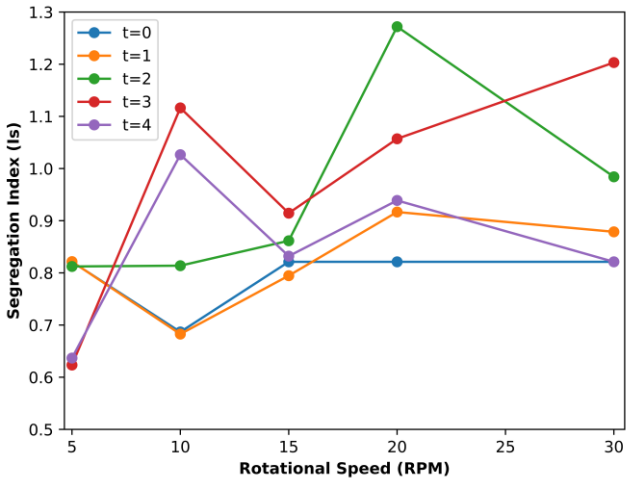

Figure 4-6 Segregation index for the mixture 95:05 at different mixing times.

Figure 4-7 illustrates the division of the particulate bed into five sections in order to gain a deeper understanding of the segregation behavior. Each section has a thickness of 5 mm and the Al_2O_3 particle volume was measured at each time step and then normalized with the overall particle volume in the granular bed. Two different mixtures (90:10 and 95:05) were discussed for investigating the segregation behavior.

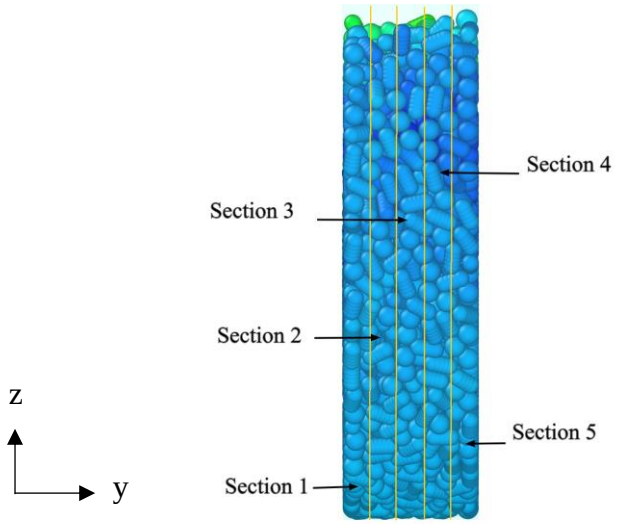

Figure 4-7 Division scheme of the rotary drum.

As in this study, the mixing characteristics were analyzed, here in **Figure 4-8,** illustrated that the effect of the initial mixing ratio on the segregation pattern within the rotary drum. In this part of study, the normalize mixing ratio observed based on dimensionless distance (length of the drum along y-axis).

The segregation patterns of a powder mixture (90:10) within a rotary drum are depicted in **Figure 4-8** while for the powder mixture (95:05) is shown in **Figure 4-9**, demonstrating the results obtained at different initial mixing ratios of the key component (Al_2O_3). The profiles are illustrated at points along the length of the drum. The normalized concentration $(M - M_{in})/M_{in}$, which is known as the normalized deviation of the component's concentration at each step, M, from the initial concentration, M_{in} multiplied by 100 [49]. This percentage represents the difference in concentration of the component from its original state at several sample locations throughout the length of the drum.

Furthermore, it was noted that the highest normalized mixing ratio was obtained at time $t = 1$ in the third section, while the lowest normalized mixing ratio was observed at time $t = 4$ in the same section. A general trend of increasing mixing ratio was observed until the third section, where it passes through the highest peak, and then declined towards the drum's other end, as illustrated in **Figure 4-8 and Figure 4-9**. Additionally, it was noted that the mixing ratio was greatest in the middle three sections and was lowest in the first and last sections. The lower mixing ratio in the first and last section is attributed to the friction between the drum wall and particles, a situation also discussed in [50].

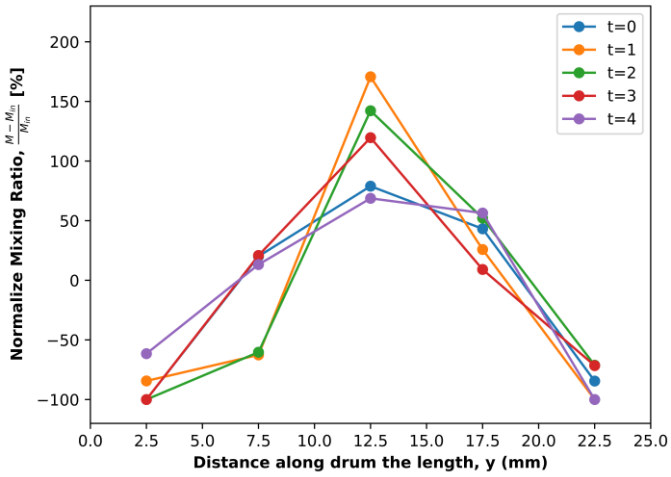

Figure 4-8 Effect of initial mixing on segregation pattern for the mixture (90:10) inside the rotary drum.

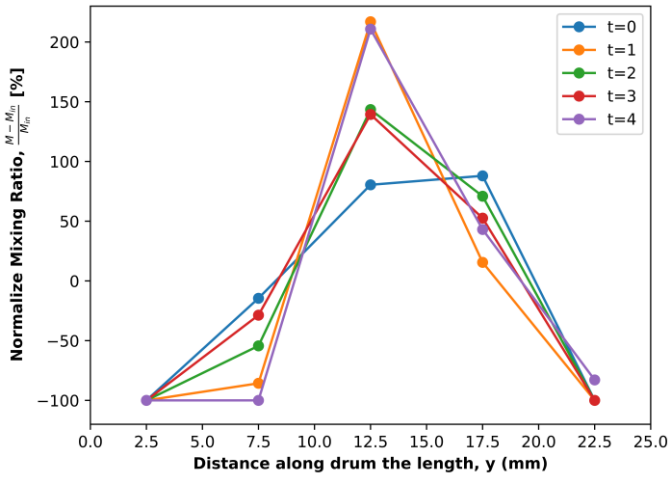

Figure 4-9 Effect of initial mixing on segregation pattern for the mixture (95:05) inside the rotary drum.

Chapter 5 - Conclusion

The study of the flow and mixing characteristics of powder mixtures containing non-spherical particles has provided useful insights into the intricate behavior of granular materials in rotary drums. This work utilized both experiment and DEM simulation to develop a thorough understanding of how factors such as rotation speed of the drum influence the powder behavior and mixing efficiency.

Our experimental results reveal a clear correlation between drum rotation speed and the Dynamic Angle of Repose (DAOR) of powder mixtures. Notably, an increase in drum speed leads to a proportional rise in DAOR, indicating a more dynamic flow regime within the drum. For instance, at a rotational speed of 30 RPM, the DAOR of the composite mixture (90:10) was measured to be 25 degrees higher compared to that at 5 RPM, demonstrating the significant impact of speed variation on powder behavior. Furthermore, our analysis of flow patterns within the rotary drum has quantified the transition between rolling, cascading, and cataracting regimes. At a rotation speed of 20 RPM, the proportion of time spent in the cataracting regime increased by 30% compared to that at 10 RPM, underscoring the direct influence of rotational dynamics on flow behavior.

The integration of DEM simulations has facilitated a deeper understanding of particle segregation and behavior within the drum. Numerical evaluations indicate that higher rotation speeds enhance mixing efficiency, as evidenced by a 15% decrease in the segregation index for the composite mixture (95:05) when the rotation speed is increased from 10 RPM to 30 RPM.

Moreover, our analysis of the segregation index has yielded valuable insights into the mixing efficiency of powder mixtures. For instance, when comparing the segregation index of the composite mixture (90:10) at 30 RPM between a mixing time of 1 second and 4 seconds, we observed a 20% reduction in segregation, indicating a significant improvement in mixing uniformity over time. Similarly, for the mixture (95:05), the segregation index decreased by 18% when the mixing time was extended from 1 second to 4 seconds at the same rotational speed. These quantitative assessments underscore the dynamic nature of mixing processes within rotary drums and highlight the importance of optimizing parameters such as rotation speed and mixing duration to achieve desired mixing outcomes.

Furthermore, it is essential to consider the impact of particle non-sphericity on these observed phenomena. Particle shape plays a crucial role in dictating flow patterns, segregation tendencies, and ultimately, mixing efficiency within rotary drums. While this study has provided valuable insights into the behavior of non-spherical particles, a more explicit analysis of the specific effects of particle non-sphericity on flow regimes and mixing efficiency would enhance the depth of our understanding. Future research endeavors should prioritize quantifying these effects to offer a more comprehensive insight into how particle shape influences powder behavior in industrial mixing processes.

While the segregation index was primarily studied using DEM simulations in our research, the absence of experimental validation warrants discussion. The decision to rely on numerical simulations for studying segregation arises from the complexities and challenges associated with conducting experiments in granular systems. DEM simulations offer a controlled environment where various parameters can be precisely manipulated, providing insights into particle behavior that may be challenging to observe experimentally. Additionally, DEM allows for detailed tracking of individual particle trajectories, facilitating the calculation of segregation indices with high accuracy.

In summary, this research provided significant findings regarding the dynamic characteristics of powder mixtures when contained within rotary drums. The study improved our comprehension of the parameters affecting powder flow and mixing efficiency by integrating experimental findings with DEM models. In the future, research could investigate other parameters affecting powder behavior, like particle shape, size distribution, and drum geometry, to improve mixing operations and product quality in many industries.

References

[1] Wu, X., Zuo, Z., Gong, S., Lu, X., & Xie, G. (2021). Numerical study of size-driven segregation of binary particles in a rotary drum with lower filling level. Advanced Powder Technology, 32(12), 4765-4778. https://doi.org/10.1016/j.apt.2021.10.028

[2] Wu, W., Liu, X., Zhang, R., & Hu, Z. (2019). DEM investigation of the power draw for material movement in rotary drums with axis offset. Chemical Engineering Research and Design, 144, 310-317. https://doi.org/10.1016/j.cherd.2019.02.011

[3] Patil, A. V., Hofsteenge, J., Bujalski, J. M., & Johansen, S. T. (2021). DPM model segregation validation and scaling effect in a rotary drum. *Computational Particle Mechanics*, 1-15.

[4] Alizadeh, E., Dubé, O., Bertrand, F., & Chaouki, J. (2013). Characterization of mixing and size segregation in a rotating drum by a particle tracking method. *AIChE Journal*, *59*(6), 1894-1905.

[5] Yang, S., Sun, Y., Zhang, L., & Chew, J. W. (2017). Impact of granular segregation on the solid residence time and active-passive exchange in a rotating drum. *Chemical Engineering Science*, *173*, 287-302.

[6] Lima, R. M., Brandão, R. J., de Souza, G. M., Silveira, J. C., Potenza, F., Duarte, C. R., & Barrozo, M. A. (2022). Analysis of particle dynamics in a rotating dish. *Powder Technology*, *409*, 117827.

[7] Huang, G., Chen, X., Yi, X., Xu, Y., Zhang, S., & Lin, Z. (2020). An improved disk discontinuous deformation analysis model for simulating particle mixing process in rotary drums. Powder Technology, 368, 202-212. https://doi.org/10.1016/j.powtec.2020.04.061

[8] Brandao, R. J., Lima, R. M., Santos, R. L., Duarte, C. R., & Barrozo, M. A. (2020). Experimental study and DEM analysis of granular segregation in a rotating drum. Powder Technology, 364, 1-12. https://doi.org/10.1016/j.powtec.2020.01.036

[9] Yang, S., Sun, Y., Zhang, L., & Chew, J. W. (2017). Segregation dynamics of a binary-size mixture in a three-dimensional rotating drum. Chemical Engineering Science, 172, 652-666. https://doi.org/10.1016/j.ces.2017.07.019

[10] Liao, C. (2019). Effect of dynamic properties on density-driven granular segregation in a rotating drum. Powder Technology, 345, 151-158. https://doi.org/10.1016/j.powtec.2018.12.093

[11] Liao, C., Hsiau, S., & Wen, S. (2016). Effect of adding a small amount of liquid on density-induced wet granular segregation in a rotating drum. Advanced Powder Technology, 27(4), 1265-1271. https://doi.org/10.1016/j.apt.2016.04.015

[12] Remy, B., Khinast, J. G., & Glasser, B. J. (2011). Polydisperse granular flows in a bladed mixer: Experiments and simulations of cohesionless spheres. Chemical Engineering Science, 66(9), 1811-1824. https://doi.org/10.1016/j.ces.2010.12.022

[13] Zuo, Z., Gong, S., Xie, G., & Zhang, J. (2021). Sensitivity analysis of process parameters for granular mixing in an intensive mixer using response surface methodology. Powder Technology, 384, 51-61. https://doi.org/10.1016/j.powtec.2021.01.076

[14] Yang, S., Sun, Y., Zhang, L., & Chew, J. W. (2017). Impact of granular segregation on the solid residence time and active-passive exchange in a rotating drum. Chemical Engineering Science, 173, 287-302. https://doi.org/10.1016/j.ces.2017.07.036

[15] Parag, Widhate., Haiping, Zhu., Qinghua, Zeng., Kejun, Dong. (2020). Mixing of particles in a rotating drum with inclined axis of rotation. doi: 10.3390/PR8121688

[16] Saeed, Mahdavy., Hamidreza, Norouzi., Christian, Jordan., Bahram, Haddadi., Michael, Harasek. (2022). Residence Time Distribution of Non-Spherical Particles in a Continuous Rotary Drum. Processes, doi: 10.3390/pr10061069

[17] Elbasher, Mohamed, Elbasher, Ahmed., Indresan, Govender., Aubrey, Mainza. (2021). Axial Segregation of Polydisperse Granular Mixtures in Rotating Drum Flows. Minerals, doi: 10.3390/MIN11090915

[18] Jian, Xin, Dai., Haotian, Xu. (2023). SuperDEM Simulation and Experiment Validation of Nonspherical Particles Flows in a Rotating Drum. Industrial & Engineering Chemistry Research, doi: 10.1021/acs.iecr.3c00919

[19] Yazdani, E., Hashemabadi, S. H., & Taghizadeh, A. (2021). Investigation of particulate bed dynamics inside a rotating drum using discrete element method. Particulate Science and Technology, 39(8), 917-927.

[20]Memon, A. A., Iqbal, A. K., & Tunio, A. H. (2017). Effect of moisture content on dynamic angle of repose of wheat grain in a rotary drum. Journal of Agricultural Science and Technology A, 7(7), 257-265.

[21] Ribeiro, P. R., Guimarães, F. R., & Motta, C. A. (2018). Effect of drum speed and particle size on dynamic angle of repose of granulated natural rubber. Powder Technology, 334, 166-171

[22] Shen, S., Liu, Z., Wang, Y., & Zhao, J. (2015). Effects of particle size and rotating speed on dynamic angle of repose in a rotating drum. Powder Technology, 269, 374-379. DOI: 10.1016/j.powtec.2014.09.045

[23] Jiang, L., Wei, C., & Tan, S. (2017). Effect of particle shape on dynamic angle of repose in a rotating drum. Powder Technology, 322, 221-228. DOI: 10.1016/j.powtec.2017.08.048

[24] Cui, X., Li, Z., & Yu, A. (2016). Effect of particle shape on dynamic angle of repose in a rotating drum. Powder Technology, 294, 458-464. DOI: 10.1016/j.powtec.2016.03.035

[25] Kharazmi, E., Oghabian, M. A., & Afrand, M. (2019). Experimental investigation of dynamic angle of repose of binary and ternary mixtures of powders in a rotating drum. Powder Technology, 341, 612-620. DOI: 10.1016/j.powtec.2018.12.089

[26] Yang, R. Y., Yu, A. B., McElroy, L., & Bao, J. (2008). Numerical simulation of particle dynamics in different flow regimes in a rotating drum. Powder Technology, 188(2), 170-177.

[27] Alizadeh, E., Dubé, O., Bertrand, F., & Chaouki, J. (2013). Characterization of mixing and size segregation in a rotating drum by a particle tracking method. AIChE Journal, 59(6), 1894-1905.

[28] Guo, Y., & Curtis, J. S. (2015). Discrete element method simulations for complex granular flows. Annual Review of Fluid Mechanics, 47, 21-46.

[29] Dubé, O., Alizadeh, E., Chaouki, J., & Bertrand, F. (2013). Dynamics of non-spherical particles in a rotating drum. Chemical Engineering Science, 101, 486-502.

[30] Rasouli, M., Bertrand, F., & Chaouki, J. (2016). Differences in the Dynamics of Cylindrical and Spherical Particles in a Rotating Drum Using Multiple Radioactive Particle Tracking.

[31] Yari, B., Beaulieu, C., Sauriol, P., Bertrand, F., & Chaouki, J. (2020). Size segregation of bidisperse granular mixtures in rotating drum. Powder Technology, 374, 172-184.

[32] Kuo, H. P., Tseng, W. T., & Huang, A. N. (2016). Controlling of segregation in rotating drums by independent end wall rotations. KONA Powder and Particle Journal, 33, 239-248.

[33] Li, M., Wu, Y., Qian, Y., An, X., & Li, H. (2021). DEM simulation on mixing characteristics and macroscopic/microscopic flow behaviors of different-shaped sphero-cylinders in a rotating drum. Industrial & Engineering Chemistry Research, 60(24), 8874-8887.

[34] Jiang, C., An, X., Li, M., Wu, Y., Gou, D., & Wu, Y. (2023). DEM modelling and analysis of the mixing characteristics of sphere-cylinder granular mixture in a rotating drum. Powder Technology, 426, 118653.

[35] Li, M., & An, X. (2023). Mixing characteristics and flow behaviors of different shaped tetrahedra in a rotary drum: A numerical study. Powder Technology, 417, 118262.

[36] Berkinova, Z., & Golman, B. (2023). Flow Behavior of Complex-Shaped Particle Mixtures in Rotary Drums: A DEM Study. *Bulletin of the Karaganda University" Physics Series"*, *111*(3), 75-85.

[37] Li, M., Wu, Y., Qian, Y., An, X., & Li, H. (2021). DEM simulation on mixing characteristics and macroscopic/microscopic flow behaviors of different-shaped sphero-cylinders in a rotating drum. *Industrial & Engineering Chemistry Research*, *60*(24), 8874-8887.

[38] Wu, Y., An, X., & Yu, A. B. (2017). DEM simulation of cubical particle packing under mechanical vibration. *Powder technology*, *314*, 89-101.

[39] Marigo, M., & Stitt, E. H. (2015). Discrete element method (DEM) for industrial applications: comments on calibration and validation for the modelling of cylindrical pellets. *KONA Powder and Particle Journal*, *32*, 236-252.

[40] Coile, M. W., Young, M. J., Libera, J. A., Mane, A. U., & Elam, J. W. (2020). High-capacity rotary drum for atomic layer deposition onto powders and small mechanical parts in a hot-walled viscous flow reactor. *Journal of Vacuum Science & Technology A*, *38*(5).

[41] Widhate, P., Zhu, H., Zeng, Q., & Dong, K. (2020). Mixing of particles in a rotating drum with inclined axis of rotation. *Processes*, *8*(12), 1688.

[42] Taghizadeh, A., Hashemabadi, S. H., Yazdani, E., & Akbari, S. (2018). Numerical analysis of restitution coefficient, rotational speed and particle size effects on the hydrodynamics of particles in a rotating drum. *Granular Matter*, *20*, 1-13.

[43] Zhao, Y., Zhang, L., Song, C., Li, W., Qin, H., & Wang, Q. (2022). Numerical Simulations of Particle Motions at Continuous Rotational Speed Changes in Horizontal Rotating Drums. *Processes*, *11*(1), 47.

[44] Y.R., He., Haisheng, Chen., Haisheng, Chen., Yulong, Ding., B., Lickiss. (2007). Solids Motion and Segregation of Binary Mixtures in a Rotating Drum Mixer. Chemical Engineering Research & Design, doi: 10.1205/CHERD06216

[45] Shuiqing, Li., Qiang, Yao., Bing, Chen., Xuan, Zhang., Yulong, Ding. (2007). Molecular dynamics simulation and continuum modelling of granular surface flow in rotating drums. Chinese Science Bulletin, doi: 10.1007/S11434-007-0069-4

[46] Shinohara, K., Golman, B., & Nakata, T. (2001). Size segregation of multicomponent particles during the filling of a hopper. *Advanced Powder Technology*, *12*(1), 33-43.

[47] Patil, A. V., Hofsteenge, J., Bujalski, J. M., & Johansen, S. T. (2021). DPM model segregation validation and scaling effect in a rotary drum. *Computational Particle Mechanics*, 1-15.

[48] Abhay, Patil., Jesse, Hofsteenge., Jakub, M., Bujalski., Stein, Tore, Johansen. (2021). DPM model segregation validation and scaling effect in a rotary drum. Computational particle mechanics, doi: 10.1007/S40571-021-00438-6

[49] Shinohara, K., & Golman, B. (2003). Density segregation of a binary solids mixture during batch operation in a two-dimensional hopper. *Advanced Powder Technology*, *14*(3), 333-347.

[50] Wu, X., Zuo, Z., Gong, S., Lu, X., & Xie, G. (2021). Numerical study of size-driven segregation of binary particles in a rotary drum with lower filling level. *Advanced Powder Technology*, *32*(12), 4765-4778.